Toward a microscopic description of dimer adsorbates on metallic surfaces

Jaime Merino,[1] László Borda,[2] and Pascal Simon[3,4]

[1]*Departamento de Física Teórica de la Materia Condensada, Universidad Autónoma de Madrid, Madris 28049, Spain*
[2]*Physikalisches Institut and Bethe Center for Theoretical Physics, Universität Bonn, Nussallee 12 D-53115 Bonn, Germany*
[3]*Department of Physics and Astronomy, University of Basel, CH-4056 Basel, Switzerland*
[4]*Laboratoire de Physique et Modélisation des Milieux Condensés, CNRS and Université Joseph Fourier, BP 166, F-38042 Grenoble, France*

(Dated: November 21, 2008)

Despite the experimental successes of Scanning Tunneling Microscopy (STM) and the interest in more complex magnetic nanostructures, our present understanding and theoretical description of STM spectra of magnetic adatoms is mainly phenomenological and most often ignores quantum many-body effects. Here, we propose a theory which includes a microscopic description of the wave functions of the substrate and magnetic adatoms together with the quantum many-body effects. To test our theory, we have computed the STM spectra of magnetic Cobalt monomers and dimers adsorbed on a metallic Copper surface and successfully compared our results to recent available experimental data.

PACS numbers: 72.15.Qm, 68.37.Ef, 72.10.Fk,75.30.Hx

Introduction In the past decade, STM experiments of magnetic adsorbates on metal surfaces have florished. They have identified sharp resonances at the Fermi surface [1, 6, 7, 8, 9], characteristic of the Kondo effect, a paradigmatic quantum many-body state which originates from the screening of the impurity spin by the conduction electrons. Systematic experimental studies of more complex structures with two or more magnetic atoms have been recently initiated and strong magnetic exchange interactions between the impurities have been identified [2, 3] and estimated [4, 5]. Despite all these important experimental successes and the interest in more complex magnetic nanostructures, our present understanding is mainly phenomenological. Since the exponentially small Kondo energy scale cannot be captured by present-day calculations based on the Density Functional Theory (DFT), a full ab initio theory of Cobalt impurities on metallic surfaces is precluded. A different strategy is therefore required. Here, we proceed in two separate steps by combining two complementary approaches: the single particle physics which is mainly responsible for the shape of the STM spectra is described by solving the Schroedinger equation in an effective potential which parameterizes the metallic surface and the adatoms while the quantum many-body physics is treated separately via the powerful numerical renormalization group (NRG) method. Such strategy captures low energy physics and should therefore be suitable to describe STM spectra of magnetic adatoms around zero bias. This constitutes a first step toward a microscopic description of competing quantum many-body states at metallic surfaces.

The Kondo effect occurs when the spin of magnetic adsorbate couples to the surrounding electrons. Below a characteristic energy scale T_K, named the Kondo temperature, the conduction electrons form a strongly-correlated singlet with the spin of the adsorbate which results in its screening. In STM experiments, this manifests as a zero-bias resonance of width T_K in the differential conductance[1, 6, 7, 8, 9]. The theoretical description of the STM spectrum of a single magnetic atom adsorbed on a metallic surface is based on a Fano line shape [10] associated with a *non-interacting* resonant level. The Fano function is most often empirically assumed while its parameters are adjusted phenomenologically [11, 12, 13, 14] or computed from a microscopic description of metal-adsorbate-tip interactions [15, 16].

When two magnetic adsorbates or more are brought into proximity, magnetic interactions between the impurities –direct or indirect– start competing with the independent screening of each impurity. From this competition different magnetic ground states can be reached [17, 18, 19] that can strongly affect the differential conductance [20] and may even lead to non-Fermi liquid behavior in small clusters [21]. In Ref. [5], Wahl *et al.* perform a systematic experimental analysis of Cobalt dimers adsorbed on a Copper surface by increasing the interatomic distance between the adatoms and therefore decreasing their magnetic exchange interactions. The measured changes of the STM spectra with the adatom interatomic distance thus permitted an indirect estimate of this coupling via STM. Below, we propose a theoretical description of low energy STM spectra of magnetic monomers and dimers adsorbed on a metallic surface by combining microscopic evaluation of the one-electron parameters with NRG calculations without making any phenomenological assumptions on the spectral shapes. We focus on Cobalt atoms adsorbed on Copper (100) to compare our results with recent experimental data by Wahl *et al.* [5] but our approach can also be extended to other magnetic adatoms and metallic surfaces.

Model We consider a cluster of N_c magnetic atoms adsorbed on a metallic surface. The complete system involves the STM tip, the substrate and can be described by the following Hamiltonian

$$H = H_{subs} + H_{tip-subs} + H_{tip}, \tag{1}$$

where H_{subs} describes the substrate plus the adsorbed 3d transition metal atom and $H_{tip-subs}$ describes the interaction of the tip with the substrate. H_{tip} describes the tip which is assumed to have an unstructured density of states. The substrate with the adsorbed 3d atom may be modeled by a generalized Anderson model. The $d_{3z^2-r^2}$ orbital is the most strongly coupled to the metal at typical adsorption distances of Co on Cu(100) due to the lobe pointing to the surface which overlaps more strongly with the metal wavefunctions. The d-orbitals parallel to the surface x-y ($d_{xy}, d_{x^2-y^2}$) plane lead to cancellations between the negative and positive lobes of the adsorbate orbital. This has been checked by evaluating the matrix elements along the lines shown in Ref. [15]. We therefore assume in the sequel that only the $d_{3z^2-r^2}$ orbital of the adatoms hybridizes with the substrate [22].

The metallic states, denoted by $|\mathbf{k}>$, couple to the $d_{3z^2-r^2}$ orbitals denoted by $|d_i>$ with $i = 1, .., N_c$ labeling each adatom of the cluster. The Anderson model usually assumes that the continuum of metal states are orthogonal to the localized orbitals of the adsorbate. However, the basis set formed by the unperturbed metal, adsorbates and tip states, $\{|\mathbf{k}>, |d_i>, |t>\}$, is generically non-orthogonal and over-complete. One way to correct this is to redefine the metallic states, $\mathbf{k}$, as:
$|\tilde{\mathbf{k}}>= |\mathbf{k}> - \sum_i < d_i|\mathbf{k}> |d_i> - < t|\mathbf{k}> |t>$. Considering that tip and adsorbate wavefunctions are orthogonal: $< t|d_i >= 0$, as $|d_i>$ is very localized, then the new metallic states satisfy $<\tilde{\mathbf{k}}|\phi>= 0$, where $|\phi>$ can be either $|t>$ or $|d_i>$.

Our starting point is thus an Anderson model defined in this new orthogonal basis: $\{|\tilde{\mathbf{k}}>, |d_i>, |t>\}$, from which associated one-electron parameters are obtained. An analogous procedure was previously used in the context of chemisorption of atoms and molecules on metal surfaces by Grimley [23]. In this basis, the substrate Hamiltonian reads

$$H_{subs} = \sum_{\mathbf{k}\sigma} \epsilon_{\tilde{\mathbf{k}}} c^\dagger_{\tilde{\mathbf{k}}\sigma} c_{\tilde{\mathbf{k}}\sigma} + \epsilon_d \sum_{j\sigma} d^\dagger_{j\sigma} d_{j\sigma} \tag{2}$$
$$+ \sum_{j=1}^{N_c} \sum_{\mathbf{k},\sigma} V_{\tilde{\mathbf{k}}j} (d^\dagger_{j\sigma} c_{\tilde{\mathbf{k}}\sigma} + H.c.) + U \sum_{j,\sigma<\sigma'} d^\dagger_{j\sigma} d_{j\sigma} d^\dagger_{j\sigma'} d_{j\sigma'}.$$

Here ϵ_d is the energy level of an electron residing in the $d_{3z^2-r^2}$ orbital of the adsorbate, $c^\dagger_{\tilde{\mathbf{k}}m\sigma}$ creates an electron with spin σ, momentum $\tilde{\mathbf{k}}$ in the metal. $d^\dagger_{j\sigma}$ creates an electron with spin σ in adsorbate-j. $\epsilon_{\tilde{\mathbf{k}}}$ and $V_{\tilde{\mathbf{k}}j}$ are the metallic energies and the hybridization matrix elements between the substrate and the adsorbate-j, respectively (notice that the momentum dependence of the hybridization matrix elements is explicitly taken into account). U is the Coulomb repulsion of two electrons in the 3d orbital of the transition metal atom. Finally, the tip-substrate interaction contribution to the Hamiltonian reads

$$H_{tip-subs} = \sum_{\mathbf{k},\sigma} M_{\tilde{\mathbf{k}}} (c^\dagger_{\tilde{\mathbf{k}}\sigma} t_\sigma + H.c.), \tag{3}$$

through the matrix elements, $M_{\tilde{\mathbf{k}}}$. Here, t_σ destroys an electron with spin σ in the tip. We have neglected the direct coupling of the tip with the substrate d bands and with the 3d orbital of the adsorbates due to the localized nature of these d orbitals.

Hybridization matrix elements In the following we briefly describe how hybridization matrix elements, $M_{\tilde{\mathbf{k}}}$ and $V_{\tilde{\mathbf{k}}}$, are computed. For simplicity we first focus on how $V_{\tilde{\mathbf{k}}}$ is computed, as $M_{\tilde{\mathbf{k}}}$ is computed in a similar way. We first re-express the Hamiltonian in Eq. (3) in first quantized form $H_{subs} = T + \sum_{j=1}^{N_c} V_j + V_M$, where T is the kinetic energy of the system, V_j is the potential created by adsorbate-j and V_M describes the surface potential. The matrix elements between the orthogonalized metallic states, $\tilde{\mathbf{k}}$, and the adsorbate thus read:

$$V_{\tilde{\mathbf{k}}j} = V_{\mathbf{k}j} - S_{\mathbf{k}j} < d_j|V_M|d_j>, \tag{4}$$

where, again, we have assumed: $< t|d_j >= 0$ and $< d_i|d_j >= \delta_{ij}$. The first term in Eq. (4) is the hybridization matrix element with the unperturbed wavefunctions $\mathbf{k}$: $V_{\mathbf{k}j} =< \mathbf{k}|V_M|d_j >$, and the second contains the overlap matrix element $S_{\mathbf{k}j} =< \mathbf{k}|d_j >$. The above orthogonalization procedure automatically selects the metal potential V_M in the hybridization matrix elements favoring the region close to or inside the metal in the integrations. This differs from hybridization matrix elements computed with the original wavefunctions as in that case integrations over the whole space are involved. The metal effective potential for the Cu(100) surface, V_M, is parameterized based on the Jones-Jennings-Jepsen (JJJ) potential [24] (see Ref. [15] for details). The sharpness of the surface barrier potential $\lambda = 2.2\text{Å}^{-1}$, and the image plane position of $Z_{im} = 1.15$ Å. The adsorbtion distance of Co on Cu(100) is estimated to be $Z_d = 1.5$ Å. Finally we note that orthogonalization effects enter the model through matrix elements only. Orthogonalization effects on the substrate band energies can be shown to be of higher order in the overlap. Hence, we assume $\epsilon_{\tilde{\mathbf{k}}} = \epsilon_{\mathbf{k}}$ in the rest of the paper.

STM conductance results Following Ref. [14] and for the sake of clarity we derive the basic equations needed for the computation of the conductance through the STM. If we neglect any modification of the substrate due to the presence of the tip (this is reasonable considering the fact that the tip is typically at about $5 - 10$ Å above the metal surface), then the differential conductance measured by the STM reads: [11, 13, 14]

$$\frac{dI}{dV}(\omega) = \frac{4e^2}{\hbar}\rho_{tip}\int d\epsilon \frac{\partial f(\epsilon-\omega)}{\partial \epsilon}(\Gamma(\epsilon)+\delta\Gamma(\epsilon)), \quad (5)$$

where $\Gamma(\omega) = \pi\sum_{\mathbf{k}}|M_{\tilde{\mathbf{k}}}|^2\delta(\omega-\epsilon_{\mathbf{k}})$ is the conductance associated with the clean substrate (without the adsorbed 3d transition metal atom) and ρ_{tip} is the density of states of the tip and $f(\epsilon)$ the Fermi-Dirac function. Modifications of the tip-surface coupling induced by the presence of the adsorbate are given by

$$\delta\Gamma(\omega) = \mathrm{Im}\sum_{i,j}\sum_{\mathbf{k},\mathbf{k}'}\frac{M_{\tilde{\mathbf{k}}}V_{\tilde{\mathbf{k}}i}}{\omega-\epsilon_{\mathbf{k}}-i\eta}G_{ij}(\omega)\frac{V^*_{j\tilde{\mathbf{k}}'}M^*_{\tilde{\mathbf{k}}'}}{\omega-\epsilon_{\mathbf{k}'}-i\eta}. \quad (6)$$

The Greens function, $G_{ij}(\omega)$, describes the electronic properties of the cluster of $3d$ adsorbates immersed in the metallic continuum including the quantum many-body effects such as the Kondo effect but also the interactions between the Co adatoms. η is an analytical continuation parameter. For convenience Eq. (6) is rewritten in the following way $\delta\Gamma(\omega) = \mathrm{Im}\sum_{i,j}\{(A_i(\omega)+iB_i(\omega))G_{ij}(\omega)(A^*_j(\omega)+iB^*_j(\omega))\}$ where $B_i(\omega) = \pi\sum_{\mathbf{k}}M_{\tilde{\mathbf{k}}}V_{\tilde{\mathbf{k}}}\delta(\omega-\epsilon_{\mathbf{k}})$ and $A_i(\omega)$ is the Kramers-Kronig transformation of $B_i(\omega)$. For the systems of interest here, $A_i(\omega)$ and $B_i(\omega)$ are real. Function $B_i(\omega)$ embodies the information concerning the tip-substrate-adsorbate system as it depends on the tip-adsorbate separation, on the position of the adsorbate with respect to the last surface plane of ions, and on the metal potential described by V_M through the matrix elements, $V_{\tilde{\mathbf{k}}i}$ and $M_{\tilde{\mathbf{k}}}$. In the single impurity case, $dI/dV(\omega)$ reduces to a Fano form[10] for $\omega < T_K$ and the line shape is determined by the Fano parameter[15]: $q = A(0)/B(0)$, evaluated at the Fermi energy taken as zero. Thus, the shape is fixed by the one-electron parameters entering the full model (1).

We apply this formalism to compute the conductance of two Co atoms deposited on Cu(100) surfaces. We take in the following the origin of distances at one of the Co adatoms in the dimer $\mathbf{R_1} = 0$ and the distance between the atoms is denoted by d. The magnetic exchange interaction depends on the interatomic distance d and is denoted as $I(d)$. This function has been calculated using *ab initio* calculations by Stepanyuk et al.[25] and also estimated experimentally [5]. Due to the small spatial range of the d orbitals compared to the typical separation between the adatoms considered here, this magnetic exchange interaction is mainly of RKKY type as it has been shown in [25]. For our purpose, we merely regard $I(d)$ as an external parameter which may eventually extracted from ab initio calculations.

The challenging task is to compute the two by two matrix G_{ij} in Eq. (6) which encodes interaction effects. In order to perform this task, we use the powerful NRG approach. However, a full NRG treatment of two five-fold degenerate impurities is a way beyond today's computational possibilities. We choose instead a simpler route and first map the Anderson Hamiltonian in Eq. (3) to a Kondo-like Hamiltonian. Such procedure is standard and justified by the fact that the electron in the $d_{3z^2-r^2}$ orbital of the Cobalt adatom is strongly bound. The resulting Kondo model is described by the two-impurity Kondo Hamiltonian [17, 18]. We neglect potential scattering terms since they do not renormalize and barely contribute to the low energy physics. The low energy physics of the two-impurity Kondo model is then controlled by only two energy scales: the single-impurity Kondo temperature T_K and the magnetic exchange interaction I [17, 18]. We use NRG calculations to obtain the impurity spectral properties.

Wilson's NRG technique [26] is a non-perturbative and numerically exact method suitable especially for quantum impurity problems (for a recent review see [27]). The cornerstone of the method is the logarithmic discretization of the conduction electron band and mapping the system onto a semi-infinite chain with the impurity at the end. NRG has been successfully applied to the problem of two magnetic impurities[18, 19] but in those earlier works only thermodynamic quantities were computed. The main source of complication in a two impurity calculation as compared to a single impurity case is that the former is an effectively two band calculation: From NRG point of view it is a challenging task because the impurities now couple to two semi-infinite chains. Consequently, the Hilbert space grows by a factor 16 in each NRG step. This is still manageable with today's computer resources. Concerning the details of the present NRG calculation, the conduction and is discretized logarithmically in intervals $[\Lambda^{n+1}D, \Lambda^n D]$ and $[-\Lambda^n D, -\Lambda^{n+1}D]$ where D is the bandwidth and Λ the discretization parameter. We took $\Lambda = 2$, the number of iterations was $N = 60$ and we kept $M = 3072$ states per iteration exploiting the charge and spin z-component $U(1)$ symmetries. The calculations were performed at $T = 0$ and $I(d)$ was taken as an input parameter we took from *ab initio* calculations [25]. In the NRG calculations, we have neglected the details of the substrate band structure and the k-dependence of the matrix elements V_{kj} since the low energy properties of the two impurity Kondo model mainly depend on the single impurity Kondo temperature and the RKKY interaction. Therefore, we expect our whole approach combining single particle description of the adsorbate together with NRG calculations to be qualitatively correct at low energies *i.e.* around zero bias and within an interval of order a few T_K. It would be interesting but quite computationally demanding to apply NRG techniques directly on the two-impurity Anderson Hamiltonian neglecting orbital degeneracy with the matrix elements V_{kj} computed from the previous single-particle calculations. We leave this for future work.

We would like to note here that in principle NRG is

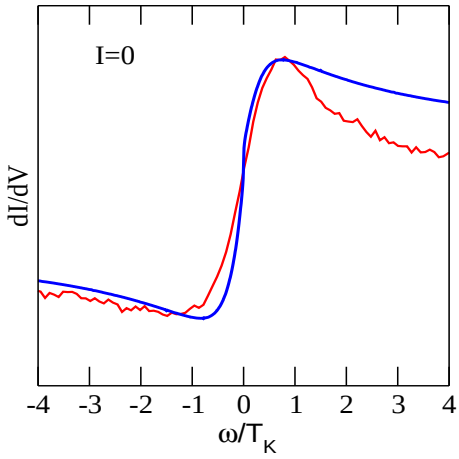

FIG. 1: Kondo resonance for a single Co adatom on a Cu(100) surface. STM measurements at T=6 K (red line) are compared to our theoretical results (black line).

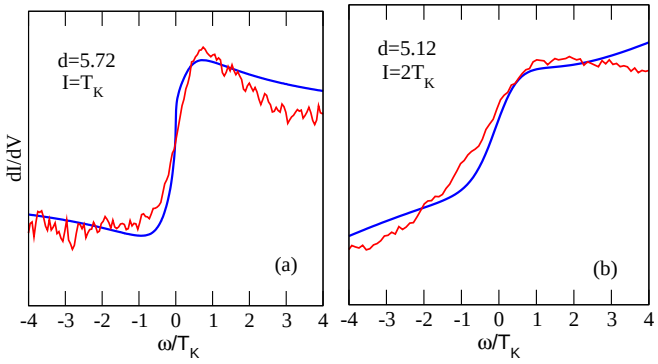

FIG. 2: Kondo resonance for Co antiferromagnetically coupled Co dimers on a Cu(100) surface. The distance, d, (in Å) between the Co atoms is reduced from (a) to (b) with the corresponding coupling $I(d)$ [25] increasing as shown. In (a) and (b) we compare theoretical calculations for an antiferromagnetic interaction, $I > 0$, and available experimental data [5] at 6 K. In (b) a linear background present in the experimental data has been appropriately added to the theoretical spectra for comparison.

capable of reproducing RKKY interaction, see Ref.[19]. Here we choose a different strategy, by mapping the problem onto two independent Wilson chains, but in contrast to Ref.[18], we take the finite overlap between the electron fields centered around the positions of the two impurities into account. In this way NRG does not generate additional RKKY interaction thus the danger of double-counting is avoided. The reason why we follow this strategy is that the RKKY interaction, generated in the NRG scheme of Ref.[19] for a Kondo-like model with constant, featureless conduction electron DoS, has a very little to do with the realistic $I(d)$ obtained by *ab initio* method.

When the two Cobalt adatoms are far apart, the RKKY interaction is negligible and the adatoms can be regarded as isolated. We have plotted in Fig. 1 the differential conductance -function of the dimensionless parameter ω/T_K- calculated using the aforementioned procedure for a single Co adatom and compared it to experimental raw data. The agreement is extremely good at low energy and qualitatively correct at higher energy.

Let us now apply the same method to obtain STM spectra for Cobalt dimers separated by a distance d such that the RKKY interaction become of the order of T_K or larger. The resulting differential conductance on top of one adatom are summarized in Figs. 2 and 3 for various distances separating the Cobalt adatoms. According to *ab initio* results [25], we can associate to the distance d=5.72 Å and d=5.12 Å the antiferromagnetic RKKY exchange interactions $I \sim T_K \approx 7.6\ meV$ and $I \sim 2T_K \approx 15.6\ meV$ respectively. We have compared in Fig. 2 our results for the conductance on top of one adatom for these two distances to the experimental raw data obtained at $T = 6K$ with a very good agreement especially at low energies. The agreement is quite remarkable since the theory contains a single fit parameter: the magnetic exchange interaction I which is extracted from *ab initio* calculations [25]). The correct shape of the STM signal is reproduced without using any Fano line shape fits which would be actually unjustified for Cobalt dimers. We then apply our method in order to predict the differential conductance for the adatom separation corresponding to d=3.5 Å and d=2.56 Å as shown in Fig. 3. The magnetic exchange interaction is predicted to be ferromagnetic [25] and corresponds to $I \approx -4T_K$) and $I \approx -46T_K$ respectively. In the latter case, the Kondo temperature is predicted to be very small, ≈ 0.23 meV and although is not accessible with present STM experiments it is the predicted line shapes resulting from our combined approach at very low temperatures.

In summary, we have presented theoretical predictions for the STM spectra of magnetic monomers and dimers adsorbed on metals. Our approach relies on a microscopic description of the adsorbate-metal-tip interactions combined with NRG calculations. Such methodology may constitute the first building block for understanding STM spectra of more complex magnetic structures on metal surfaces.

Acknowledgment We acknowledge P. Wahl and K. Kern for discussions and for sending us their raw data files for the Cobalt dimers adsorbed on Cu(100). J.M. thanks O. Gunnarsson for useful comments on the manuscript. L.B. acknowledges the financial support of the Alexander von Humboldt Foundation, János Bolyai Foundation and Hungarian Grants OTKA through projects T048782 and K73361.

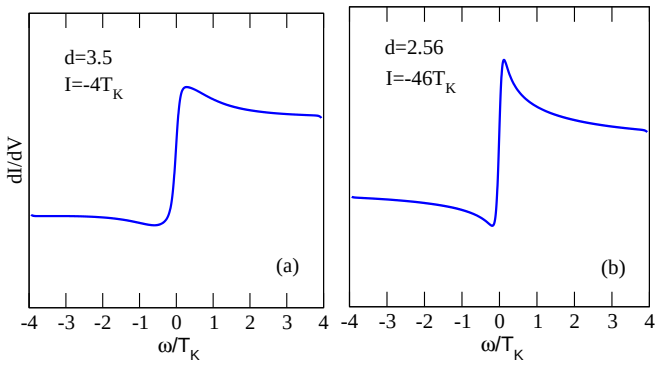

FIG. 3: Kondo resonance for ferromagnetically coupled dimers on a Cu(100) surface. Experimental data do not show a Kondo effect at 6 K for d=2.56 Å, which is in agreement with the strong reduction in the Kondo temperature predicted here.

[1] H. C. Manoharan, C. P. Lutz, and D. M. Eigler, Nature (London) **403**, 512 (2000).

[2] W. Chen, T. Jamneala, V. Madhavan, and M. F. Crommie, Phys. Rev. B **60**, 8529 (1999).

[3] T. Jamneala, V. Madhavan, and M. F. Crommie, Phys. Rev. Lett. **87**, 256804 (2001).

[4] C. F. Hirjibehedin, C. P. Lutz, and A. J. Heinrich, Science **312**, 1021 (2006).

[5] P. Wahl *et al.*, Phys. Rev. Lett. **98**, 056601 (2007).

[6] V. Madhavan, W. Chen, T. Jamneala, M. F. Crommie, and N. S. Wingreen, Science **280**, 567 (1998).

[7] J. Li, W.-D. Schneider, R. Berndt, and B. Delley, Phys. Rev. Lett. **80**, 2893 (1998).

[8] N. Knorr, M. A. Schneider, L. Diekhoner, P. Wahl, and K. Kern, Phys. Rev. Lett. **88**, 096804 (2002).

[9] N. Néel, J. Kröger, L. Limot, K. Palotas, W. A. Hofer, and R. Berndt, Phys. Rev. Lett. **98**, 016801 (2007)

[10] U. Fano, Phys. Rev. **124**, 1866 (1961).

[11] A. Schiller and S. Hershfield, Phys. Rev. B **61**, 9036 (2000).

[12] O. Újsághy, J. Kroha, L. Szunyogh, and A. Zawadowski, Phys. Rev. Lett. **85** 2557 (2000).

[13] M. Plihal and J. Gadzuk, Phys. Rev. B **63**, 085404 (2001).

[14] V. Madhavan, W. Chen, T. Jamneala, M. F. Crommie, and N. S. Wingreen, Phys. Rev. B **64** 165412 (2001).

[15] J. Merino and O. Gunnarsson, Phys. Rev. B **69**, 115404 (2004); Phys. Rev. Lett. **93** 156601 (2004).

[16] C.-Y. Lin, A. H. Castro Neto, and B. A. Jones, Phys. Rev. Lett. **97**, 156102, (2006); Phys. Rev. B **71**, 035417 (2005).

[17] B.A. Jones, C.M. Varma, Phys. Rev. Lett. **58**, 843 (1987).

[18] B.A. Jones, C.M. Varma, and J.W. Wilkins *ibid.* **61**, 125 (1988).

[19] J. B. Silva, W. L. C. Lima, W. C. Oliveira, J. L. N. Mello, L. N. Oliveira, and J. W. Wilkins Phys. Rev. Lett. **76**, 275 (1996)

[20] P. Simon, R. Lopez, and Y. Oreg, Phys. Rev. Lett. **94** 086602 (2005).

[21] B. Lazarovits, P. Simon, G. Zaránd, and L. Szunyogh, Phys. Rev. Lett. **95**, 077202 (2005); K Ingersent, A. W. Ludwig, and I. Affleck, Phys. Rev. Lett. **95**, 257204 (2005).

[22] M. Weissmann and A. M. Llois, Phys. Rev. B **63**, 113402 (2001).

[23] T. B. Grimley, *Molecular processes on Solid Surfaces*, edited by E. Drauglis, R. D. Gretz, and R. I. Jaffee (McGraw-Hill, New York, 1969), p. 299.

[24] R. O. Jones, P. J. Jennings, and O. Jepsen, Phys. Rev. B **29**, 6474 (1984).

[25] V. Stepanyuk, A. Baranov, D. Bazhanov, W. Hergert, A. Kastelson, Surface Science **482-485**, 1045 (2001).

[26] K. G. Wilson, Rev. Mod. Phys. **47**, 773 (1975).

[27] R. Bulla, T. A. Costi, T. Pruschke, Rev. Mod. Phys. **80**, 395 (2008).